Journal of Molecular Graphics and Modelling 49 (2014) 18–24

Contents lists available at ScienceDirect

Journal of Molecular Graphics and Modelling

journal homepage: www.elsevier.com/locate/JMGM

Identification of p38α MAP kinase inhibitors by pharmacophore based virtual screening

Rahul P. Gangwal[a], Nihar R. Das[b], Kaushik Thanki[c], Mangesh V. Damre[a], Gaurao V. Dhoke[a], Shyam S. Sharma[b], Sanyog Jain[c], Abhay T. Sangamwar[a,*]

[a] Department of Pharmacoinformatics, National Institute of Pharmaceutical Education and Research (NIPER), Sector-67, S.A.S. Nagar, Punjab 160 062, India
[b] Department of Pharmacology and Toxicology, National Institute of Pharmaceutical Education and Research (NIPER), Sector-67, S.A.S. Nagar, Punjab 160 062, India
[c] Centre for Pharmaceutical Nanotechnology, Department of Pharmaceutics, National Institute of Pharmaceutical Education and Research (NIPER), S.A.S. Nagar (Mohali), Phase X, Sector-67, Punjab 160 062, India

ARTICLE INFO

Article history:
Received 14 November 2013
Accepted 2 January 2014
Available online 13 January 2014

Keywords:
Cytotoxicity
Molecular docking
p38 MAP kinase
Pharmacophore modeling
Virtual screening

ABSTRACT

The p38α mitogen-activated protein (MAP) kinase plays a vital role in treating many inflammatory diseases. In the present study, a combined ligand and structure based pharmacophore model was developed to identify potential DFG-in selective p38 MAP kinase inhibitors. Conformations of co-crystallised inhibitors were used in the development and validation of ligand and structure based pharmacophore modeling approached. The validated pharmacophore was utilized in database screening to identify potential hits. After Lipinski's rule of five filter and molecular docking analysis, nineteen hits were purchased and selected for *in vitro* analysis. The virtual hits exhibited promising activity against tumor necrosis factor-α (TNF-α) with 23–98% inhibition at 10 μM concentration. Out of these seven compounds has shown potent inhibitory activity against p38 MAP kinase with IC_{50} values ranging from 12.97 to 223.5 nM. In addition, the toxicity study against HepG2 cells was also carried out to confirm the safety profile of identified virtual hits.

1. Introduction

Cytokine targeting has become an important focus in the treatment of many inflammatory disorders such as rheumatoid arthritis [1], inflammatory bowel disease [2], Crohn's disease [3] and psoriasis [4,5]. p38 mitogen activated protein (MAP) kinase is the key agitator in acclimation to biosynthesis and release of pro-inflammatory cytokines [6]. Four variants of p38 MAP kinase have been documented, namely, p38α (also known as p38), p38β, p38γ (ERK6/SAPK3) and p38δ (SAPK4) with 40–60% structural similarity [7–10], while the roles of p38β, p38γ and p38δ have yet to be identified [11]. In response to a variety of stress stimuli (heat, UV light, lipopolysaccharide, high osmolarity), p38 MAP kinase gets activated *via* dual phosphorylation of the TGY motif in the activation loop of the enzyme. Upon activation, it phosphorylates some downstream substrates, thereby regulates the synthesis of several important pro-inflammatory cytokines such as tumor necrosis factor-α (TNF-α) and interleukin-1 (IL-1) [12]. Therefore, p38 MAP kinase inhibition would potentially prevent the underlying pathophysiology of the inflammatory diseases, making it an attractive target for drug discovery [13–15].

In recent studies, it has been reported that most inhibitors (type I inhibitors) target the ATP binding site, which contains the conserved Phe residue of the Asp-Phe-Gly (DFG) motif buried in a hydrophobic pocket between the two lobes of the p38 MAP kinase [16,17]. Another set of inhibitors (type II) occupies the ATP binding site along with the allosteric pocket, which appears to be accessible only when the Phe side chain of the DFG motif moves out from the hydrophobic pocket [18]. Data from an X-ray, kinetic and cellular study provides the detailed comparison of potent compounds from the same chemical series that binds to DFG-in and DFG-out conformations [19]. Unexpectedly, type II inhibitors that are bound to the DFG-out conformation have shown diminished selectivity [20–24]. However, some type I inhibitors (*e.g.*, VX-745) that bind to the DFG-in conformation have shown very specific selectivity toward the p38 MAP kinase [25].

We are primarily focusing on identification of potent and selective inhibitors (type I) based on the bioactive conformation of inhibitors from the protein data bank, which can correctly reflect the structure–activity relationship (SAR) of the existing p38 MAP kinase inhibitors. Structure and ligand based pharmacophore modeling approaches were combined and applied to achieve this goal. The best qualitative pharmacophore model (Comb_Hypo1) was

* Corresponding author. Tel.: +91 172 2214682.
E-mail addresses: abhays@niper.ac.in, abhaysangamwar@gmail.com (A.T. Sangamwar).

1093-3263/$ – see front matter © 2014 Elsevier Inc. All rights reserved.
http://dx.doi.org/10.1016/j.jmgm.2014.01.002

generated and used as a 3D query to screen Specs, NCI and ChemDiv databases. The hits were subsequently filtered by Lipinski's rule of five and docking studies. Further, obtained hits were evaluated for TNF-α and p38 MAP kinase inhibition. Finally, seven compounds with diverse scaffolds were reported as possible candidates for the design of potent p38 MAP kinase inhibitors.

2. Materials and methods

2.1. Data sets

The most important step in the pharmacophore modeling is the selection of suitable training set, responsible for determining the quality of the generated pharmacophore. In last few decades, more than 166 crystal structures of p38 MAP kinase were reported in the protein data bank. Out of these, 152 protein structures were obtained from Homo sapiens. The inhibitory activity for 65 out of 142 co-crystallized p38 MAP kinase inhibitors was reported in the protein data bank. From these 37 co-crystal structures having DFG-in conformation of p38 MAP kinase were aligned in PyMOL1.4.1 [26] and ligands were extracted for further pharmacophore studies. The inhibitory activities of extracted inhibitors were expressed in terms of the IC_{50} value (*i.e.*, the half maximal inhibitory concentration, a measure of the effectiveness of a compound in inhibiting biological or biochemical function), which spanned across a wide range from 0.8 nM to 1 mM [27].

2.2. Pharmacophore modeling

Combined structure and ligand based pharmacophore modeling approach is a fruitful tool in drug discovery to discover the compounds with improved potency. All the pharmacophore modeling studies were carried out using Common Feature Pharmacophore Generation and Ligand Pharmacophore Mapping protocols within Accelrys Discovery Studio2.5 (DS2.5) software package [28] and LigandScout3.0 [29] on IBM graphics workstation.

2.2.1. Ligand based approach

Five co-crystallized inhibitors were used as training set to develop common feature pharmacophore using DS2.5. As we have considered the protein bound conformations of the inhibitors in the training set, no prior diverse conformation generation step was performed to generate diverse conformations. All training set molecules have been extracted from their crystal structures and verified for their bond orders. Minimum inter-feature distance value was set to 2 Å so that the functional groups located close to each other were also considered during pharmacophore generation. The 'MaxOmitFeat' and 'Principal' values were set to 0 and 2, respectively, for all training set compounds as we have included only most active compounds. Hydrogen bond acceptor (HBA), hydrogen bond donor (HBD), hydrophobic (HY) and ring aromatic (RA) features were selected based on the chemical features of compounds in the training set using Feature Mapping protocol available in DS2.5 and the proposed mechanism of action. Rests of the parameters were set at their default values. Ten pharmacophore hypotheses were produced using Common Feature Pharmacophore Generation protocol, and the best one (Hypo1) was selected for further studies based on the rank, best-fit values and the interaction points available at the active site.

2.2.2. Structure based approach

From the available crystal structures of p38 MAP kinase, twelve were selected based on the IC_{50} values of their inhibitors and crystal structure resolutions for the generation of structure based pharmacophore models. The interaction between ligand and amino acids present in the active site has provided sufficient input to generate the structure based pharmacophore. LigandScout3.0, an automated tool for pharmacophore generation was used to study the interaction between the inhibitors and amino acids in the active site of p38 MAP kinase. It identifies protein ligand interactions such as hydrogen bond, charge transfer, hydrophobic regions, and also defines excluded volume spheres based on the side chain atoms to characterize the inaccessible areas for any potential ligand. All generated structure based pharmacophore hypotheses were exported in .hypoedit format and then converted into .chm format using Hypoedit tool in DS2.5 and subsequently used as 3D query for the screening process.

2.2.3. Validation of pharmacophore model

The validation of developed pharmacophore model was done to determine whether it is capable of identifying active and inactive compounds and further performing virtual screening of databases [30]. To validate the generated pharmacophore hypotheses two kinds of data set were constructed, test set and decoy set. Test set contains 25 diverse compounds extracted from co-crystallized p38 MAP kinase having DFG-in conformation. The activity values (IC_{50}) of test compounds were classified into the active ($IC_{50} < 2500$ nM) and least active ($IC_{50} \geq 2500$ nM) inhibitors. As we have considered the protein bound conformations of the test set inhibitors, diverse conformation generation step was not performed to generate diverse conformations. The compounds for decoy set were obtained from a Directory of Useful Decoys (DUD database) [31]. 19 active p38 MAP kinase inhibitors were included in the decoy set to calculate various statistical parameters such as goodness of hit score (GH) and enrichment factor (*E* value). GH score and *E* value are two major parameters, which plays an important role in identifying the capability of the generated pharmacophore hypothesis.

2.3. Virtual screening

Virtual screening of chemical databases helps in finding novel and potential leads suitable for further development [32]. Fast/Flexible and Best/Flexible are the two database searching options available in DS2.5. In our study, we performed virtual screening using Best/Flexible search option. The validated pharmacophore model (Comd_Hypo1) was used as 3D query in database screening. Three commercially available databases of diverse chemical compounds were used in virtual screening. Maximum Omitted Features option was set to '0' to screen the databases. Hits were screened for Fit values and then checked for their drug-likeness properties using Lipinski's rule of five. Those which passed all of these tests were taken for molecular docking analysis.

2.4. Molecular docking

To investigate the detailed intermolecular interactions between the virtual hits and p38 MAP kinase, an automated docking program Glide5.5 [33] was used. Three-dimensional structure information of the target protein was taken from the protein data bank (PDB ID: 2RG6). The energy minimized conformation of the co-crystallized ligand (287) was docked into p38 MAP kinase to validate the docking protocol. The results show that the docking simulations reproduce the crystal complexes very well with root mean squared deviation (RMSD) of 0.6108 Å. The protocol followed for docking studies of virtual hits included the processing of the protein and ligand. During protein preparation, ligand molecules were deleted, hydrogen atoms were added, solvent molecules were deleted; and bond orders for crystal protein were adjusted and minimized up to 0.30 Å RMSD. An active site of 10 Å was created around the co-crystallized ligand. Standard precision (SP) mode and other default parameters of Glide software were used for the docking studies.

Table 1
Top ten pharmacophore hypotheses generated using HIPHOP for p38 MAP kinase Inhibitors.

Hypothesis name	Features[a]	Rank	Direct hit	Partial hit	Max. fit
Hypo1	HY, HY, HBA, HBA, HBA	60.682	11111	00000	5
Hypo2	HY, HY, HBA, HBA, HBA	60.517	11111	00000	5
Hypo3	RA, HY, HBA, HBA, HBA	60.175	11111	00000	5
Hypo4	RA, HY, HBA, HBA, HBA	60.175	11111	00000	5
Hypo5	HY, HY, HBA, HBA, HBA	56.682	11111	00000	5
Hypo6	HY, HY, HBA, HBA, HBA	56.517	11111	00000	5
Hypo7	HY, HY, HBA, HBA	56.182	11111	00000	4
Hypo8	RA, HY, HBA, HBA	55.270	11111	00000	4
Hypo9	HY, HY, HBA, HBA	52.182	11111	00000	4
Hypo10	HY, HY, HBA, HBA	52.182	11111	00000	4

[a] HY, hydrophobic; HBA, hydrogen bond acceptor; RA, ring aromatic.

2.5. Biological evaluation

2.5.1. LPS-induced TNF-α production in MCF-7 cells

MCF-7 cells, grown in tissue culture flasks and maintained in 5% CO_2 atmosphere at 37 °C, were used for cell culture experiments. The cell medium was supplemented with Dulbecco's modified Eagle's culture medium (DMEM), 20% fetal bovine serum (FBS), 100 U/ml penicillin, and 100 mg/ml streptomycin. The cells were harvested in 0.25% trypsin–EDTA solution (Sigma) once 90% confluence in the cell culture medium was attained. The cells were then cultured in a 96-well plate (Costars, Corning Incorporated) at a density 50,000 cells/well and incubated overnight for cell attachment to proceed for subsequent studies. Seeded cells were washed with PBS and then incubated at 37 °C with different concentrations of screened virtual hits for 2 h followed by LPS induction for 12 h. The cells were fixed after various treatments. The TNF-α concentration in the medium was measured by specific enzyme-linked immunosorbent assay using human TNF-α kit according to the manufacturer's instructions (Krishgen bio systems, Mumbai). Recombinant human TNF-α was used as a standard in this assay.

2.5.2. p38α MAP kinase in vitro assay

The Ray Bio® cell-based p38 MAPK ELISA kit (USA) was used for measuring the relative amount of p38 MAPK (Thr180/Tyr182) in cultured cells. Manufacturer's instruction was followed in the above assay. Briefly, the cells were seeded into a 96-well tissue culture plate using poly-L-lysine. After washing with PBS, the cells were incubated at 37 °C with different concentration of screened virtual hits for 1 h followed by LPS induction for 12 h. The cells were fixed after various treatments. After blocking, anti-p38 MAPK (primary antibody) is pipetted into the wells and incubated. The wells are washed, and HRP-conjugated anti-mouse IgG (secondary antibody) is added to the wells. The wells are washed again, a TMB substrate solution is added to the wells and color developed in proportion to the amount of protein. The Stop Solution changed the color from blue to yellow, and the intensity of the color was measured at 450 nm.

2.5.3. MTT assay

HepG2 cells, grown in 25 cm^2 tissue culture flasks and maintained in 5% CO_2 at 37 °C, were used for cell culture experiments. The cell medium was supplemented with Dulbecco's modified Eagle's culture medium (DMEM), 20% fetal bovine serum (FBS), 100 U/ml penicillin, and 100 mg/ml streptomycin. The cells were harvested in 0.25% trypsin–EDTA solution (Sigma) once 90% confluence in the cell culture medium was attained. The cells were then cultured in a 96-well plate (Costars, Corning Incorporated) at a density 50,000 cells/well and incubated overnight for cell attachment to proceed for subsequent studies.

The cultured cells, washed with Hank's buffered salt (HBS) solution (PAA, Austria) for three times, were taken for MTT assay. After removing the HBS solution from the plates, cells were incubated with 0.2 ml of fresh DMEM containing free-screened virtual hits at concentrations of 10 μM for 24 h. Cell viability was then determined by MTT assay. Briefly, cells were washed with HBS solution and incubated again with 0.2 ml fresh DMEM containing 0.5 mg/ml MTT (Sigma, USA) for 3 h. The medium was then removed and MTT formazan was dissolved in 0.2 ml dimethylsulfoxide. The optical density was then determined at 550 nm using an ELISA plate reader (BioTek, USA).

3. Results and discussion

3.1. Generation of pharmacophore models

The reported crystal structures of p38 MAP kinase from the protein data bank were analyzed for organism source, conformations, bound inhibitors and their activity. Finally, 37 co-crystal structures having DFG-in conformation of p38 MAP kinase were selected for pharmacophore mapping studies. Prior to pharmacophore modeling studies, the binding site analysis was performed for better understanding of the specificity and pharmacophore requirement of inhibitors (Table S1). The binding site was characterized by several direct interactions such as hydrogen bond interactions, cation-π interaction and lipophilic side chain complement, which reflects the hydrophobic nature of an active site. One hydrogen bond interaction with Met109 and cation-π interaction with Lys53 has been shown by most of the inhibitors. The inhibitors having IC_{50} less than 4 nM were showing additional hydrogen bonds interaction with Glu71. Some of the potent inhibitors were also showing the additional π–π interaction with Tyr35.

The selected co-crystal structures having DFG-in conformation were aligned and ligands were extracted for ligand-based pharmacophore mapping studies. Five co-crystallized inhibitors (PDB ID: 2RG6, 2RG5, 3GFE, 3BX5 and 3ITZ) were selected as training set molecules (Figure S1) based on the binding site analysis, which were showing additional hydrogen bond interaction with Glu71 and $IC_{50} \leq 4$ nM. The qualitative top ten HipHop hypotheses were generated based on the training set molecules to identify the structural and chemical features necessary for inhibiting p38 MAP kinase. Table 1 summarizes the generated pharmacophore hypotheses with their statistical parameters. Direct and partial hit mask value of '1′ and '0′ indicated that the molecules were well mapped to all the chemical features in the hypothesis and there is no partial mapping or missing features respectively. The generated hypotheses consist of either four or five of pharmacophore features (HBA, HY and RA); which vary in their composition, orientation and vector directions. In the developed pharmacophore hypotheses, HBA features were representing the hydrogen bond interaction with the Met109 and Asp168, whereas HY feature representing the cation-π interaction with Lys53. Hypo1 was selected as the best qualitative pharmacophore model based on the chemical feature

similarities, ranking score and their corresponding geometric constrains. Hypo1 consists of three HBA and two HY features, which were present in all the training set molecules. It was good enough to map all the training set compounds, which inhibit the p38 MAP kinase at nanomolar level but the necessary hydrophobic features for inhibitory activity were not generated in Hypo1. Thus pharmacophore hypotheses based on the active site was necessary to identify and include the complimentary features that will facilitate inhibitory activity.

For structure based pharmacophore studies, we have used LigandScout3.0, which provides the interactions between protein and ligand as well as some excluded volume spheres corresponding to their 3D structures of protein. We have used twelve p38 MAP kinase bound conformation co-ordinates having PDB ID: 2RG6, 2RG5, 3GFE, 3BX5, 3ITZ, 1ZZL, 3HLL, 1OZ1, 1YQJ, 2I0H, 2QD9 and 1OVE for structure based pharmacophore hypothesis generations. These structures were selected based on the resolution (<2.5 Å) and IC_{50} values (<20 nM). Comparing the twelve pharmacophore models, one HBA from most of the models was pointed toward Met109, which plays a major role in p38 MAP kinase inhibitory activity. Hence HBA was considered as important chemical feature to discover the p38 MAP kinase inhibitors. The dynamic structure based pharmacophore was generated by superimposing the twelve structure based hypotheses generated from co-crystallized protein structures. During this, over lapping features were considered and extra features were deleted [34]. Finally, five featured dynamic structure based hypothesis (SB_Hypo1) was obtained, which consists of one HBA and four HY features.

The pharmacophore Hypo1 and SB_Hypo1 were found to be significant in the test set prediction. However, both pharmacophore models were non-selective and tend to capture too many false-positive hits during the decoy set validation. Hence, we have aligned both pharmacophores with RMSD of 0.0745 using pharmacophore comparison tool in DS2.5. Finally, a merged pharmacophore hypothesis (Comb_Hypo1) was generated by removing overlapping features. The Comb_Hypo1 consists of three HBA and four HY features. Figure S2 shows the chemical features of pharmacophore hypotheses (Hypo1, SB_Hypo1, and Comb_Hypo1) with their inter-feature distance constraints.

3.2. Pharmacophore models validation

The test set prediction was employed as first process in validation of the developed pharmacophore hypotheses. Hypo1, SB_Hypo1 and Comb_Hypo1 were used to estimate the FitValue of test set compounds. Table S2 summarizes the diverse pharmacophore hypotheses compositions and their hit rate against active and inactive compounds. The Comb_Hypo1 model showed the superior hit rates than the other models. The best pharmacophore query Comb_Hypo1 was comprised of three hydrogen bond acceptors, and four hydrophobic features. In detail, 16 of 17 highly active and 8 of 8 inactive compounds were predicted correctly by the Comb_Hypo1. One active compound was underestimated as inactive. The most active in the test set mapped over Comb_Hypo1 (Fig. 1a) showed that five features were being mapped accurately. While in the case of the least active compound, two HBA and two HY features were missing (Fig. 1b).

Finally, a small database (D) containing 9160 compounds, which includes 19 active and 9141 inactive p38 MAP kinase inhibitors were used to validate whether the hypotheses (Hypo1, SB_Hypo1 and Comb_Hypo1) could discriminate actives from inactive compounds. Database screening was performed using developed pharmacophore hypotheses, as a 3D structural query. 94.73, 63.15 and 89.47% of active compounds from the decoy set were successfully retrieved by Hypo1, SB_Hypo1, and Comb_Hypo1, respectively. For the analysis of decoy set screening results, enrichment factor (*E*-value) and goodness of hit score (GH) were calculated using the following formulae.

$$E = \frac{H_a \times D}{H_t \times A} \tag{1}$$

$$\mathrm{GH} = \frac{H_a}{4H_tA}(3A + H_t) \times \left(1 - \frac{H_t - H_a}{D - A}\right) \tag{2}$$

where D, A, H_t and H_a represent the total number of compounds of the database, total number of actives, total number of compounds found by a pharmacophore model and total number of active compounds screened, respectively [35,36]. In addition, Hypo1, SB_Hypo1 and Comb_Hypo1 have shown an E value of 15.09, 6.28 and 390.27 respectively. The calculated GH scores for Hypo1 (0.244) and SB_Hypo1 (0.138) were less than 0.5, which indicate that the quality of developed pharmacophore models was not significant. While in case of Comb_Hypo1, the calculated GH score was greater than 0.5 (0.830), which indicates that the quality of Comb_Hypo1 was significant (Table 2). From the overall validation results, we assure that Comb_Hypo1 hypothesis was able to discriminate between the active and inactive or low active compounds. Hence, we have used Comb_Hypo1 hypothesis for virtual screening to select or discriminate suitable p38 MAP kinase inhibitors.

3.3. Sequential virtual screening

The sequential virtual screening was performed as depicted in the flowchart (Fig. S3). The validated merged pharmacophore model (Comb_Hypo1) was used as a query to search the NCI, ChemDiv and Specs databases, which comprised of 87,374, 843,113 and 276,807 compounds, respectively. 3846 hit compounds were

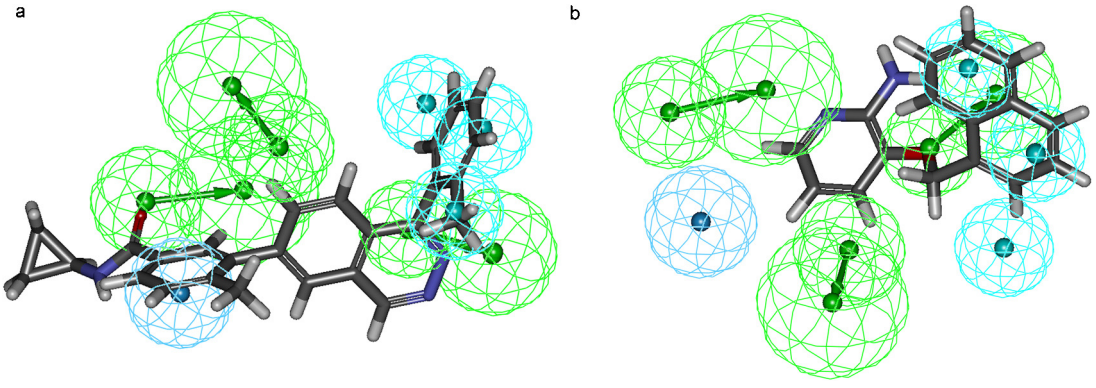

Fig. 1. (a) The most active compound from test set aligned with a merged pharmacophore model (Comb_Hypo1). (b) The least active compound from test set aligned with a merged pharmacophore model (Comb_Hypo1). Hydrogen bond acceptor indicated as green-vectored spheres and hydrophobic features indicated as cyan spheres.

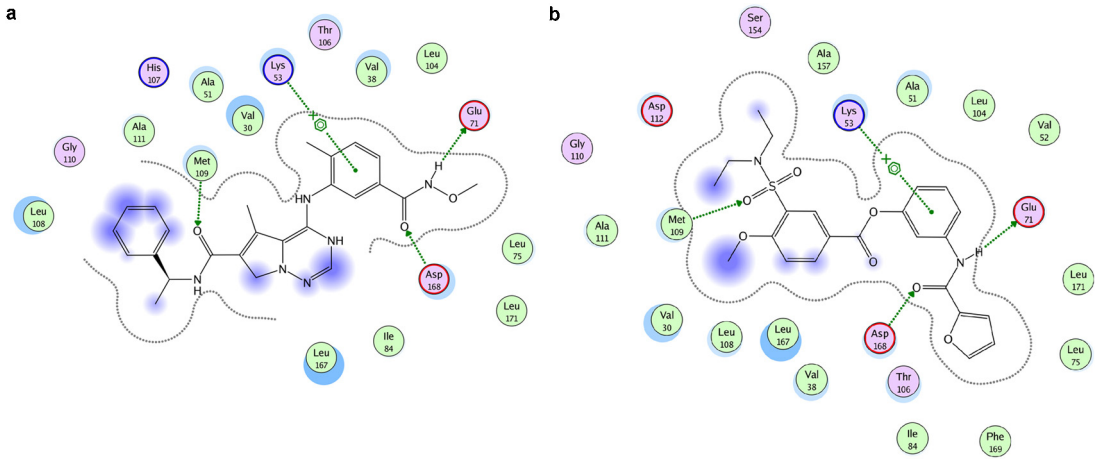

Fig. 2. (a) 2D interaction map of co-crystallized ligand (287) with the active site of p38 MAP kinase. (b) 2D interaction map of top virtual hit (ZINC00991000) with the active site of p38 MAP kinase (PDB ID: 2RG6).

mapped to the pharmacophore model, which included some structurally similar compounds to that of existing p38 MAP kinase inhibitors and some novel scaffolds were also identified. A set of 701 hit compounds were selected based on the estimated FitValue and submitted further for evaluation by Lipinski's rule of five. On applying above-mentioned filters, we obtained 198 hit compounds from 701 compounds, which have shown drug-like properties. The hit compounds were exported as sdf file and subjected to further analysis by molecular docking studies to avoid the false-positive hits from virtual screening.

3.4. Molecular docking studies

The molecular docking studies were carried out to explore the interaction mechanism between virtual hits and the receptor. All the virtual hits were docked into the active site of p38 MAP kinase using Glide program. Glide score, which differentiates compounds based on their interaction pattern is calculated for all the molecules. The most active co-crystallized ligand of training set (287) has shown the glide score of −8.972, while top virtual hit (ZINC00991000) has shown the glide score of −8.209. The co-crystallized ligand has exhibited various hydrogen-bonding interactions with the active site amino acid residues, which were as shown in Fig. 2a. The top virtual hits were showing similar binding pattern as to that of the co-crystallized ligand. Fig. 2b shows the docking pose of top virtual hit compound into the active site of p38 MAP kinase. Two hydrogen-bond interactions between backbone NH of Asp168 with the amide carbonyl and side chain of Glu71 with the amide NH of all inhibitors and screen top virtual hit were conserved. It was also observed that the sulphonyl oxygen of phenylsulphonamide group of top virtual hit forms a hydrogen bond with NH backbone of Met109. It has also shown one cation-π interaction with Lys53. The binding interaction patterns observed during docking studies were complementary with that of the hydrogen bond acceptor and hydrophobic features of the pharmacophore hypotheses. On the basis of molecular docking analysis, nineteen virtual hits (Fig. S4) with different scaffold were selected as potential p38 MAP kinase inhibitors. Further, search by PubChem and SciFinder scholar search tools confirmed that these compounds were not reported as p38 MAP kinase inhibitors. Hence, we suggest that these virtual hits will serve as lead for designing of potent p38 MAP kinase inhibitors.

3.5. Biological evaluation

The hits obtained from p38 MAP kinase pharmacophore based virtual screening were initially evaluated for % TNF-α inhibition using human TNF-α ELISA kit. Recombinant human TNF-α was used as standard. Table 3 lists the biological assay results, indicating that seven compounds (6, 9, 2, 13, 14, 18 and 19) showed moderate TNF-α inhibitory activity (60.1–77%). Compounds 3, 10 and 11 have showed least TNF-α inhibitory activity (<50%). The nine compounds (1, 4, 5, 7, 8, 12, 15, 16 and 17) have showed high % TNF-α inhibition at 1 μM. Out of these eight compounds, showing high % TNF-α inhibition (>80%), were selected for further evaluation of p38 MAP kinase inhibitory activity.

The hits were evaluated using Ray Bio® cell-based p38 MAPK ELISA kit (USA). SB203580, a known p38 MAP kinase inhibitor was used as a standard. Table 3 lists the p38 MAP kinase inhibitory activity (nM) for selected eight screened virtual hits. Out of eight, five compounds (1, 5, 7, 15 and 17) have shown higher inhibitory activity in comparison to known standard compound (SB203580). Compound 4 has shown least activity (783.9 nM).

Table 2
The statistical parameters obtained from Decoy test.

Sr. no.	Parameter	Hypo1	SB_Hypo1	Comb_Hypo1
1	Total compounds in database (D)	9160	9160	9160
2	Total number of actives in database (A)	19	19	19
3	Total hits (H_t)	575	921	21
4	Active hits (H_a)	18	12	17
5	% Yield of actives	94.73	63.15	89.47
6	% Ratio of actives in the hit list	3.13	1.30	80.95
7	Enrichment factor or enhancement (E)	15.09	6.28	390.27
8	False negatives ($A - H_a$)	1	7	2
9	False positives ($H_t - H_a$)	557	909	4
10	GH score (goodness of hit list)	0.244	0.138	0.830

Table 3
Anti-inflammatory activity against TNF-α and p38α MAP kinase.

Sr. no.	Compound	%TNF-α inhibition at 10 μM	p38α MAP kinase IC_{50} (nM)
1	ZINC00991000	93.08	33.88
2	ZINC01063326	68.51	NA
3	ZINC02861798	48.21	NA
4	ZINC09251689	87.53	783.9
5	ZINC00653168	98.00	57.23
6	ZINC00831033	72.15	NA
7	ZINC15784950	91.26	12.97
8	ZINC21662469	83.25	NA
9	ZINC18525886	70.97	NA
10	ZINC00652427	23.00	NA
11	ZINC09723003	35.29	NA
12	ZINC08604910	93.08	223.5
13	ZINC08961134	62.96	NA
14	ZINC15861078	63.59	NA
15	ZINC08809597	80.80	36.63
16	ZINC12364825	93.08	NA
17	ZINC00682085	77.70	67.70
18	ZINC08617286	63.59	NA
19	ZINC09250456	56.77	NA
20	SB203580	NA	80.0

Some of the p38 MAP kinase inhibitors were withdrawn from clinical trial due to hepatotoxicity [37], so we have selected HepG2 cells to perform the cytotoxicity studies. The HepG2 cells were exposed to obtained hits at 10 μM concentration for 24 h and cytotoxicity was determined with the MTT assay. All the compounds have shown higher than 90% cell viability, which suggest that screened compounds are non-cytotoxic to HepG2 cells.

4. Conclusions

We have combined structure and ligand based pharmacophore modeling approaches followed by sequential virtual screening and molecular docking studies to identify p38 MAP kinase inhibitors. The screened hits have shown potent inhibitory activity against TNF-α and p38 MAP kinase. Thus, identified hits may serve as lead for developing potential candidates for inflammatory disorders such as rheumatoid arthritis, inflammatory bowel disease, Crohn's disease and psoriasis. Also, the pharmacophore modeling approach applied here will serve as guideline in the identification of lead for other targets in drug discovery process.

Acknowledgement

The authors acknowledge financial support from Department of Science and Technology (DST), New Delhi.

Appendix A. Supplementary data

Supplementary data associated with this article can be found, in the online version, at http://dx.doi.org/10.1016/j.jmgm.2014.01.002.

References

[1] M.L. Foster, F. Halley, J.E. Souness, Potential of p38 inhibitors in the treatment of rheumatoid arthritis, Drug News Perspect. 13 (2000) 488–497.
[2] P. Rutgeerts, G. D'Haens, S. Targan, E. Vasiliauskas, S.B. Hanauer, D.H. Present, L. Mayer, R.A. Van Hogezand, T. Braakman, K.L. DeWoody, Efficacy and safety of retreatment with anti-tumor necrosis factor antibody (infliximab) to maintain remission in Crohn's disease, Gastroenterology 117 (1999) 761–769.
[3] A.M. Badger, J.N. Bradbeer, B. Votta, J.C. Lee, J.L. Adams, D.E. Griswold, Pharmacological profile of SB 203580, a selective inhibitor of cytokine suppressive binding protein/p38 kinase, in animal models of arthritis, bone resorption, endotoxin shock and immune function, J. Pharmacol. Exp. Ther. 279 (1996) 1453–1461.
[4] M. Feldmann, F.M. Brennan, R.N. Maini, Role of cytokines in rheumatoid arthritis, Annu. Rev. Immunol. 14 (1996) 397–440.
[5] R.P. Gangwal, A. Bhadauriya, M.V. Damre, G.V. Dhoke, A.T. Sangamwar, p38 mitogen-activated protein kinase inhibitors: a review on pharmacophore mapping and QSAR studies, Curr. Top. Med. Chem. 13 (2013) 1015–1035.
[6] N.C. Romeiro, M.G. Albuquerque, R.B. Alencastro, M. Ravi, A.J. Hopfinger, Construction of 4D-QSAR models for use in the design of novel p38-MAPK inhibitors, J. Comput. Aided Mol. Des. 19 (2005) 385–400.
[7] Y. Jiang, C. Chen, Z. Li, W. Guo, J.A. Gegner, S. Lin, J. Han, Characterization of the structure and function of a new mitogen-activated protein kinase (p38), J. Biol. Chem. 271 (1996) 17920–17926.
[8] S. Kumar, P.C. McDonnell, R.J. Gum, A.T. Hand, J.C. Lee, P.R. Young, Novel homologues of CSBP/p38 MAP kinase: activation, substrate specificity and sensitivity to inhibition by pyridinyl imidazoles, Biochem. Biophys. Res. Commun. 235 (1997) 533–538.
[9] Y. Jiang, H. Gram, M. Zhao, L. New, J. Gu, L. Feng, F. Di Padova, R.J. Ulevitch, J. Han, Characterization of the structure and function of the fourth member of p38 group mitogen-activated protein kinases p38, J. Biol. Chem. 272 (1997) 30122–30128.
[10] R.G. Kulkarni, P. Srivani, G. Achaiah, G.N. Sastry, Strategies to design pyrazolyl urea derivatives for p38 kinase inhibition: a molecular modeling study, J. Comput. Aided Mol. Des. 21 (2007) 155–166.
[11] R. Newton, N. Holden, Inhibitors of p38 mitogen-activated protein kinase: potential as anti-inflammatory agents in asthma, BioDrugs 17 (2003) 113–129.
[12] P.S. Ambure, R.P. Gangwal, A.T. Sangamwar, 3D-QSAR and molecular docking analysis of biphenyl amide derivatives as p38α mitogen activated protein kinase inhibitors, Mol. Divers. 16 (2012) 377–388.
[13] F.M. Brennan, M. Feldmann, Cytokines in autoimmunity, Curr. Opin. Immunol. 8 (1996) 872–877.
[14] G. Camussi, E. Lupia, The future role of anti-tumour necrosis factor (TNF) products in the treatment of rheumatoid arthritis, Drugs 55 (1998) 613–620.
[15] S.J. Pollack, K.S. Beyer, C. Lock, I. Müller, D. Sheppard, M. Lipkin, D. Hardick, P. Blurton, P.M. Leonard, P.A. Hubbard, A comparative study of fragment screening methods on the p38 kinase: new methods, new insights, J. Comput. Aided Mol. Des. 25 (2011) 677–687.
[16] Y. Liu, N.S. Gray, Rational design of inhibitors that bind to inactive kinase conformations, Nat. Chem. Biol. 2 (2006) 358–364.
[17] C. Pargellis, L. Tong, L. Churchill, P.F. Cirillo, T. Gilmore, A.G. Graham, P.M. Grob, E.R. Hickey, N. Moss, S. Pav, Inhibition of p38 MAP kinase by utilizing a novel allosteric binding site, Nat. Struct. Biol. 9 (2002) 268–272.
[18] M.A. Bogoyevitch, D.P. Fairlie, A new paradigm for protein kinase inhibition: blocking phosphorylation without directly targeting ATP binding, Drug Discov. Today 12 (2007) 622–633.
[19] R.M. Angell, T.D. Angell, P. Bamborough, M.J. Bamford, C. Chung, S.G. Cockerill, S.S. Flack, K.L. Jones, D.I. Laine, T. Longstaff, Biphenyl amide p38 kinase inhibitors 4: DFG-in and DFG-out binding modes, Bioorg. Med. Chem. Lett. 18 (2008) 4433–4437.
[20] J. Bain, L. Plater, M. Elliott, N. Shpiro, C.J. Hastie, H. McLauchlan, I. Klevernic, J.S.C. Arthur, D.R. Alessi, P. Cohen, The selectivity of protein kinase inhibitors: a further update, Biochem. J. 408 (2007) 297–315.
[21] P. Bamborough, D. Drewry, G. Harper, G.K. Smith, K. Schneider, Assessment of chemical coverage of kinome space and its implications for kinase drug discovery, J. Med. Chem. 51 (2008) 7898–7914.
[22] M.A. Fabian, W.H. Biggs, D.K. Treiber, C.E. Atteridge, M.D. Azimioara, M.G. Benedetti, T.A. Carter, P. Ciceri, P.T. Edeen, M. Floyd, A small molecule-kinase interaction map for clinical kinase inhibitors, Nat. Biotechnol. 23 (2005) 329–336.
[23] O. Fedorov, B. Marsden, V. Pogacic, P. Rellos, S. Müller, A.N. Bullock, J. Schwaller, M. Sundstrom, S. Knapp, A systematic interaction map of validated kinase inhibitors with Ser/Thr kinases, PNAS 104 (2007) 20523–20528.
[24] D.M. Goldstein, N.S. Gray, P.P. Zarrinkar, High-throughput kinase profiling as a platform for drug discovery, Nat. Rev. Drug Discov. 7 (2008) 391–397.
[25] M.W. Karaman, S. Herrgard, D.K. Treiber, P. Gallant, C.E. Atteridge, B.T. Campbell, K.W. Chan, P. Ciceri, M.I. Davis, P.T. Edeen, A quantitative analysis of kinase inhibitor selectivity, Nat. Biotechnol. 26 (2008) 127–132.
[26] PyMOL 1.4.1, Molecular Graphics System, DeLano Scientific LLC, San Carlos, CA, USA, 2011.
[27] http://www.rcsb.org/pdb/home/home.do
[28] Discovery Studio Version 2.5, User Manual, Accelrys Inc., San Diego, CA, 2009.
[29] LigandScout 3.0, Inte:Ligand GmbH, Clemesn-Maria-Hofbaurer-G.6, 2344, Maria Enzersdorf, Austria, 2010.
[30] N. Bharatham, K. Bharatham, K.W. Lee, Pharmacophore identification and virtual screening for methionyl-tRNA synthetase inhibitors, J. Mol. Graphics Modell. 25 (2007) 813–823.
[31] http://dud.docking.org/
[32] S. Sakkiah, S. Thangapandian, S. John, Y.J. Kwon, K.W. Lee, 3D QSAR pharmacophore based virtual screening and molecular docking for identification of potential HSP90 inhibitors, Eur. J. Med. Chem. 45 (2010) 2132–2140.
[33] Glide 5.5, Schrödinger, LLC, 120 West 45th Street, New York, NY 10036, 2009.
[34] G.V. Dhoke, R.P. Gangwal, A.T. Sangamwar, A combined ligand and structure based approach to design potent PPAR-alpha agonists, J. Mol. Struct. 1028 (2012) 22–30.

[35] U. Singh, R.P. Gangwal, G.V. Dhoke, R. Prajapati, A.T. Sangamwar, 3D QSAR pharmacophore-based virtual screening and molecular docking studies to identify novel matrix metalloproteinase 12 inhibitors, Mol. Simul. 39 (2012) 385–396.
[36] M. Lalit, R.P. Gangwal, G.V. Dhoke, M.V. Damre, K. Khandelwal, A.T. Sangamwar, A combined pharmacophore modelling, 3D-QSAR and molecular docking study of substituted bicyclo-[3.3.0]oct-2-enes as liver receptor homologue-1 (LRH-1) agonists, J. Mol. Struct. 1049 (2013) 315–325.
[37] D.M. Goldstein, T. Gabriel, Pathway to the clinic: inhibition of P38 MAP kinase. A review of ten chemotypes selected for development, Curr. Top. Med. Chem. 5 (2005) 1017–1029.